RJC

RASĀYAN *J. Chem.*
Vol. 9 | No. 4 |556 - 565 | October - December | 2016
ISSN: 0974-1496 | e-ISSN: 0976-0083 | CODEN: RJCABP
http://www.rasayanjournal.com
http://www.rasayanjournal.co.in

INFLUENCE OF Fe_3O_4 NANOPARTICLES DISPERSED IN LIQUID CRYSTALLINE COMPOUNDS: SPECTROSCOPIC CHARACTERIZATION

J.Sivasri[1], M.C.Rao[2], G.Giridhar[3], B.T.P.Madhav[4], T.E.Divakar[5] and R. K.N.R. Manepalli[1*]

[1]Department of Physics, The Hindu College, Krishna University, Machilipatnam-521001, India
[2]Department of Physics, Andhra Loyola College, Vijayawada-520008, India
[3]Department of Nanotechnology, Acharya Nagarjuna University, Guntur-522510, India
[4]LCRC-R&D, Department of ECE, K. L. University, Guntur-522502, India
[5]Department of Chemistry, Noble College, Machilipatnam-521001, India
*E-mail: manepalli.67@gmail.com

ABSTRACT

The synthesis is carried on liquid crystalline (LC)p-decyloxy benzoic acid (10OBA) and p-undecyloxy benzoic acid (11OBA) with 0.5wt % and1wt% for Fe_3O_4 nanoparticles dispersion. The prepared samples are characterized by different spectroscopic techniques like X-ray diffraction (XRD), Scanning Electron Microscopy (SEM), Fourier Transform Infra Red (FTIR) and Differential Scanning Calorimetry (DSC). Textural determinations of the synthesized compounds are recorded by using Polarizing Optical Microscope (POM) attached with a hot stage and camera. The results show that the dispersion of Fe_3O_4 nanoparticles in 10OBA and 11OBA exhibits NC phases as same as the pure 10OBA and 11OBA with reduced clearing temperature as expected. Further, the nematic thermal range is increased in both 10OBA and 11OBA with Fe_3O_4 nanoparticles dispersion.

Keywords: Synthesis, POM, DSC, Nano-dispersion, XRD, FTIR and SEM.

INTRODUCTION

Liquid crystals are self-assembled functional soft materials which possess both order and mobility at molecular, supra-molecular and macroscopic levels[1-3]. Liquid crystals are attractive materials, since they show unique properties, such as long-range order, cooperative effects and an anisotropic nature in optical and electronic properties, based on a self-organizing nature in a certain temperature range with fluidity[4]. Owing to the possible synergetic relationship with nanomaterials, liquid crystals can play a very significant role in nanoscience and nanotechnology. Nanoparticles can be utilized to regulate and organize liquid crystal molecules in a systematic manner to achieve different phase manner under optimum environmental conditions. Nanoscale particles do not induce significant distortion in LC phases. Therefore, different nanomaterials are dispersed and studied in LC media to enhance the physical properties of LCs[5]. Moreover, alignment and self-assembly of nanomaterials themselves can be achieved in LC phases[6]. The key point for all the possible applications is the alignment of liquid crystal molecules (i.e. the director) on the substrate[7,8].

LCs act as tunable solvents for the dispersion of nanomaterials and LCs being anisotropic media, they provide a very good support for the self-assembly of nanomaterials in to large organized structures in multiple dimensions. Hence LC mediated self-assembly can be efficiently used to organize different kinds of nanomaterials in to soft and well defined functional super structures. Nano-objects (guests) that are embedded in the liquid crystals (hosts) can trap ions, which decrease the ion concentration and electrical conductivity and improve the electro-optical response of the host[9].

The variation in optical texture, electro-optic and dielectric properties of iron oxide nanoparticles embedded ferroelectric liquid crystal with respect to change in temperature and electrical bias conditions.

Incorporation of iron oxide nanoparticles makes it easier to get better profile of display parameters[10].Fe_3O_4 nanoparticles inspire researcher's new researchable ideas; this is due to its characteristics, which has a great significance in various fields. Fe_3O_4 nanoparticles have attracted much interest not only in the field of magnetic recording media such as audio and videotape and high-density digital recording disks, magnetic fluids, data storage, but also in the areas of medical care such as drug delivery systems (DDS), medical applications, including radiofrequency hyperthermia, photomagnetics and magnetic resonance imaging (MRI), medical diagnostics and cancer therapy and microwave devices, magneto-optics devices, sensors, high frequency applications, catalysis and magnetic sensing[11-21].In the present work, we reported the dispersion of Fe_3O_4 nanoparticles into LCs and analyzed by using SEM and XRD. Furthermore, the influence of nanoparticles has affected the thermal ranges of LCs which was analyzed by POM and DSC.

EXPERIMENTAL

LC compounds such as 10OBA and 11OBA and Fe_3O_4 nanoparticles are brought from Sigma-Aldrich laboratories, USA and used as such. For uniform dispersion of nanoparticles in 10OBA and 11OBA, the nanoparticles are first dissolved in ethyl alcohol, stirred well about 45 minutes and later introduced in the isotropic state of mesogenic material (10OBA/11OBA) in the ratio of 0.5wt% and 1 wt% concentration separately. After cooling, the nanocomposite 10OBA and 11OBA[22] is subjected to study of the textural and phase transition temperatures using a polarizing optical microscope (SDTECHS make) with a hot stage in which the substance was filled in planar arrangement in 4 µm cells and these could be placed along with the thermometer described by Gray[23]. Textural and phase transition temperatures are studied after preparation of the sample and observations are made again to understand the stability of Fe_3O_4 nanoparticles. A DSC (Perkin Elmer Diamond DSC) is used to obtain the transition temperatures and the enthalpy values.BRUKER-ALPHA FTIR spectrometer is used for the present study. The presence of Fe_3O_4 nanoparticles in 10OBA and 11OBA are studied by SEM data and existence as well as grain size is determined by XRD technique.

RESULTS AND DISCUSSION

Phase transition temperatures and phase sequence of the compounds has been presented by POM and confirmed by DSC. The existence of dispersed nanoparticles and their size determined by FTIR, XRD and SEM techniques.

Polarizing Microscope Studies

The transition temperatures and textures observed by POM in pure 10OBA is shown in Fig.-1a, Fig.-1b and Fig.-1c while that of 10OBA with dispersed 0.5 wt% of Fe_3O_4 nanoparticles shown in Fig.-2a, Fig.-2b andFig.-2c and that of 11OBA pure is shown in Fig.-3a, Fig.-3b and Fig.-3c while that of 11OBA with dispersed 0.5wt% of Fe_3O_4 nanoparticles shown in Fig.-4a, Fig.-4b and Fig.-4c respectively. The thermal ranges of nematic and Smectic phases are changed slightly due to the dispersion of nanoparticles and the textures of the phase's changes by the self-assembly of nanoparticles. Thermal nematic ranges are increased with increase of concentration of Fe_3O_4 nanoparticles in pure LCs.

The thermal analysis studies performed from the technique such as DSC provides data regarding the temperatures, heats of transition and heat capacities of different phases (Table-1).DSC reveals the presence of phase transitions in a material by detecting the enthalpy change associated with each phase transition, precise phase identifications cannot be made. The level of enthalpy change involved at the phase transition does provide some indication of the types of phase involved. DSC is used in conjunction with optical polarizing microscopy to determine the mesophase types exhibited by a material.

Thermograms of 10OBA and 11OBA with 0.5 wt % and 1 wt % Fe_3O_4 nanoparticles dispersion are shown in Fig.-5, Fig.-6, Fig.-7 and Fig.-8.From the DSC thermogram with the dispersion of Fe_3O_4 nanoparticles, it is observed that the enthalpy change decreases at every phase transition when compared with the pure LC. This occurs due to the presence of the Fe_3O_4 nanoparticles with the interaction of LC molecules.

POM Textures of 10OBA Pure

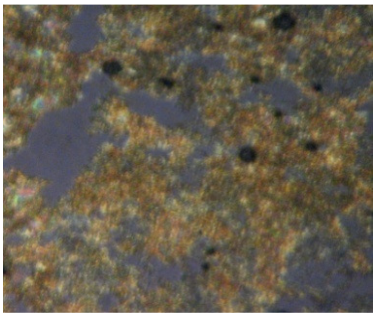

(a.) Nematic at 138.9 ºC

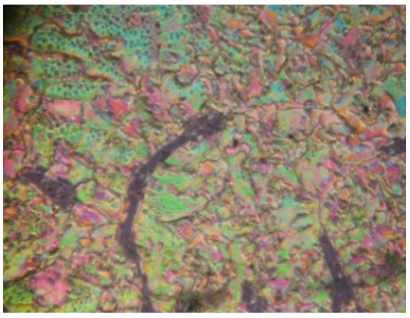

(b.) Smectic c at 122.8 ºC

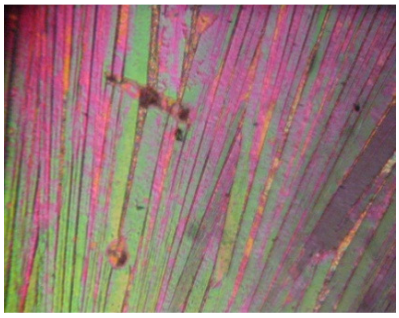

(c.) Solid at 85.5 ºC

Fig.-1

POM Textures of 10OBA + 0.5% Fe_3O_4

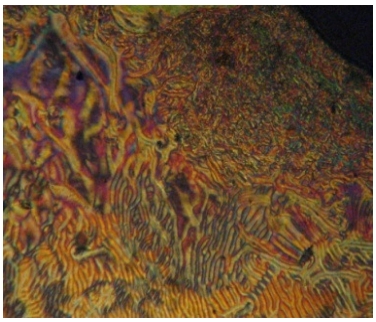

(a.) threaded Nematic

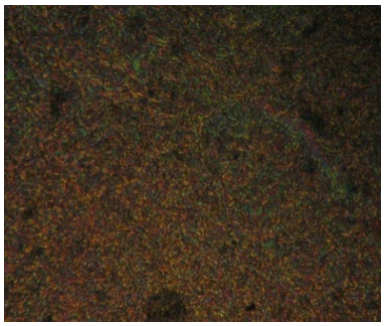

(b.) Smectic c at 116.8 ºC

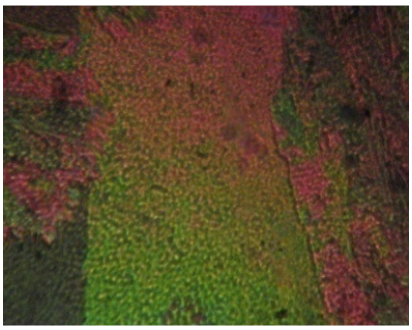

(c.) Solid at 88 ºC

Fig.-2

POM Textures of 11OBA Pure

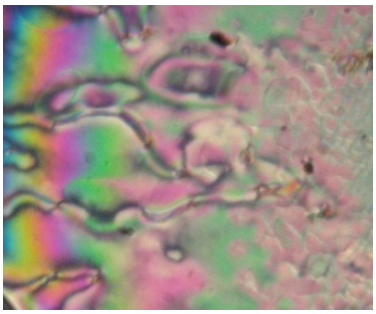

(a.)Nematic marble at 137.4 ºC

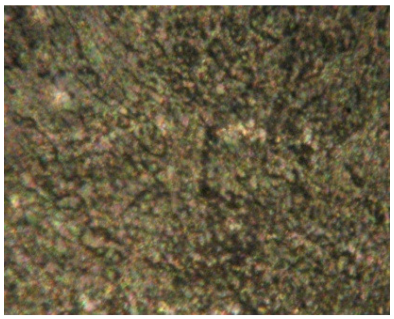

(b.)Smectic c at 126.3 ºC

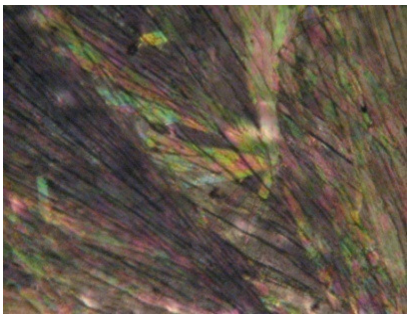

(c.)Solid at 85.4 ºC

Fig.-3

POM Textures of 11OBA + 0.5% Fe_3O_4

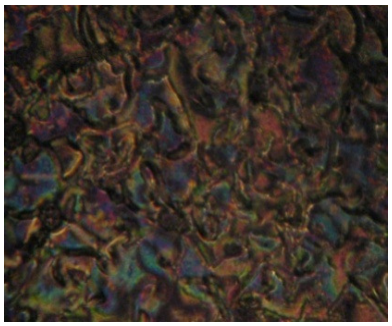

(a.)Nematic at 135.0 ºC

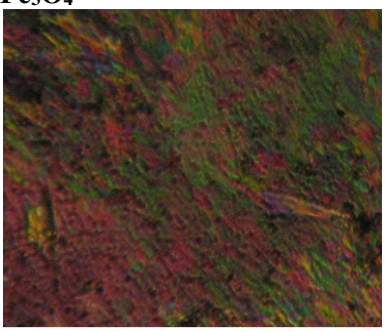

(b.)Smectic c at 122.2 ºC

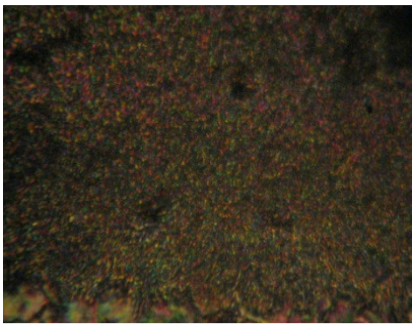

(c.)Solid at 80.5 ºC

Fig.-4

Table-1: Phase variants, transition temperatures, enthalpy values of 10OBA and 11OBA pure and with dispersed 0.5wt% and 1wt% Fe_3O_4 nanoparticles

S.No.	Compound	DSC/ POM	Scan Rate	Transition Temperatures °C				Thermal Ranges	
				I-N	N-SmC	SmC-Solid I	SolidI - Solid II	ΔN	ΔSmC
1	10OBA PURE	DSC	20c/min ΔHJ/g	138.45 2.39	121.97/ 92.56 1.55/108 2	87.06 0.11	72.54	16.48	34.91
		POM		138.9	122.8	85.5	60.2	16.1	37.3
2	10OBA+ 0.5wt% Fe_3O_4	DSC	20c/min ΔHJ/g	135.77 7.65	117.65 3.59	88.66 29.75	64.47 21.98	18.12	28.99
		POM		135.96	116.8	88.0	63.8	19.16	28.8
3	10OBA+ 1 wt% Fe_3O_4	DSC	20c/min ΔHJ/g	133.81 9.38	109.45 2.32	80.95 33.02		24.36	28.5
		POM		133.0	109.2	78.1	66.4	23.8	31.1
4	11OBA PURE	DSC	20c/min ΔHJ/g	137.1 4.76	126.3 4.32	85.2 23.01	71.8 14.97	10.8	41.1
		POM		137.4	126.3	85.4	71	11.1	40.9
5	11OBA+ 0.5wt% Fe_3O_4	DSC	20c/min ΔHJ/g	135.2 4.97	122.6 3.75	81.0 20.84	69.2 14.94	12.6	41.6
		POM		135.0	122.2	80.5	69.0	12.8	41.7
6	110BA+ 1wt% Fe_3O_4	DSC	20c/min ΔHJ/g	131.54 6.30	117.06 2.93	77.07 20.13	67.42 8.21	14.48	39.99
		POM		132.5	117.2	76.9	66.5	15.3	40.3

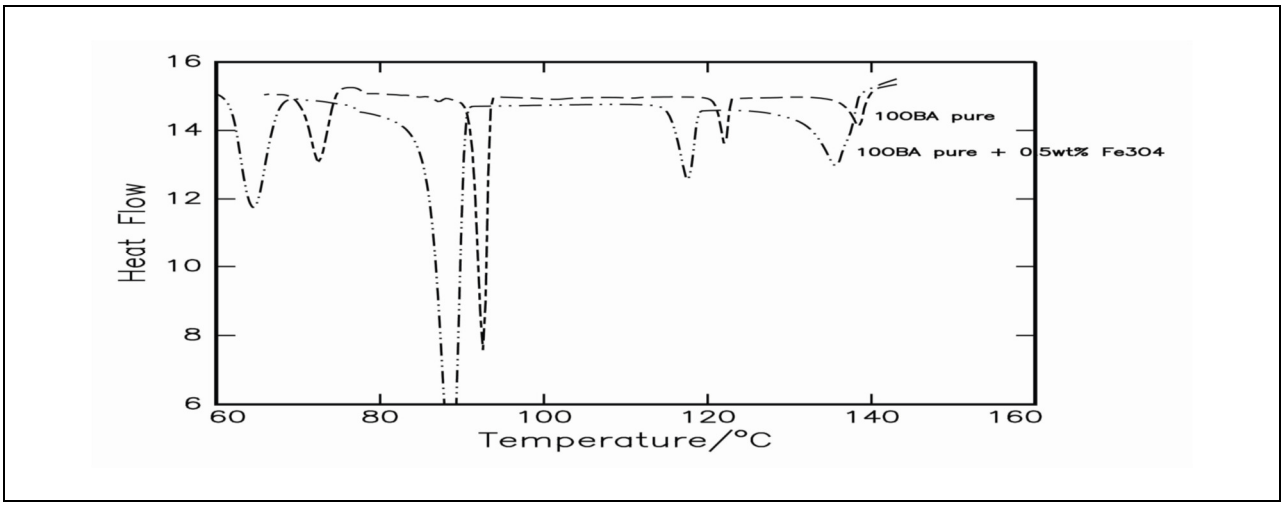

Fig.-5: DSC Thermogram of 10OBA Pure and 10OBA + 0.5wt% Fe_3O_4

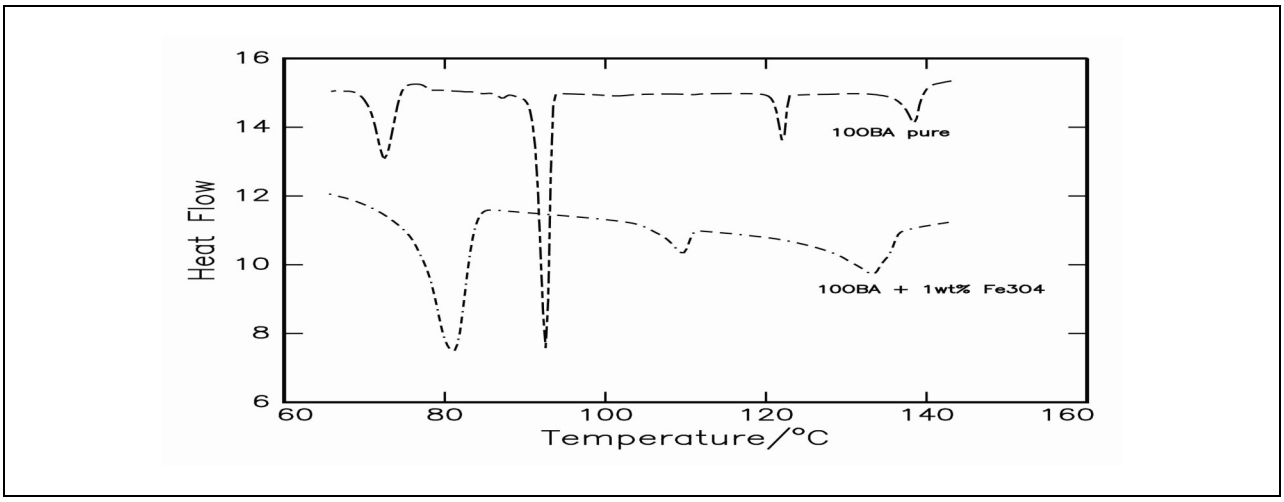

Fig.-6: DSC Thermogram of 10OBA pure and 10OBA+ 1wt% Fe_3O_4 nanoparticles

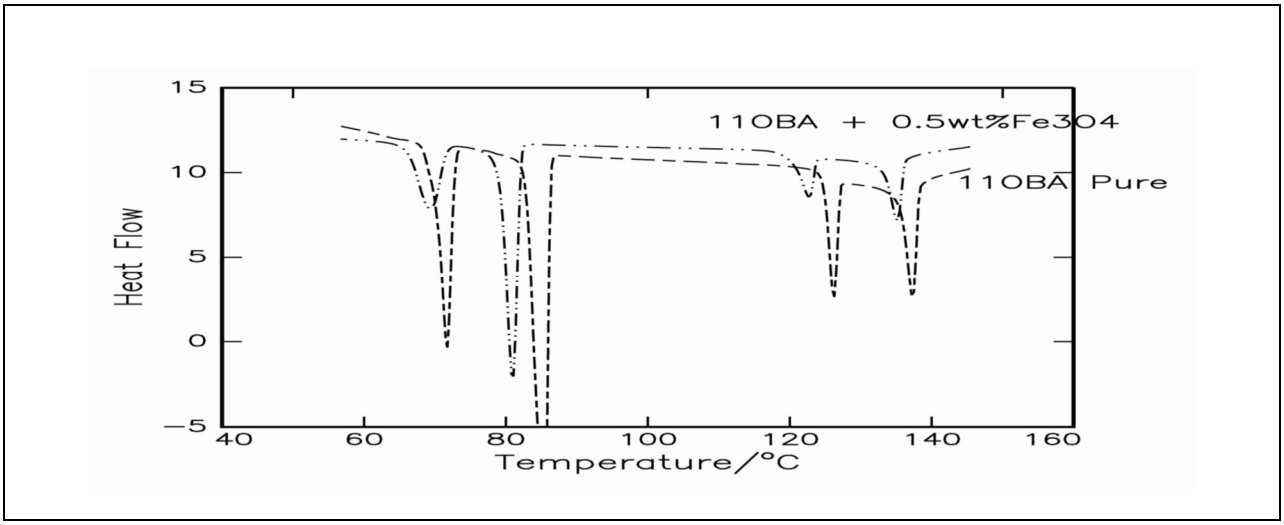

Fig.-7: DSC Thermogram of 11OBA pure and 11OBA+ 0.5wt% Fe_3O_4 nanoparticles

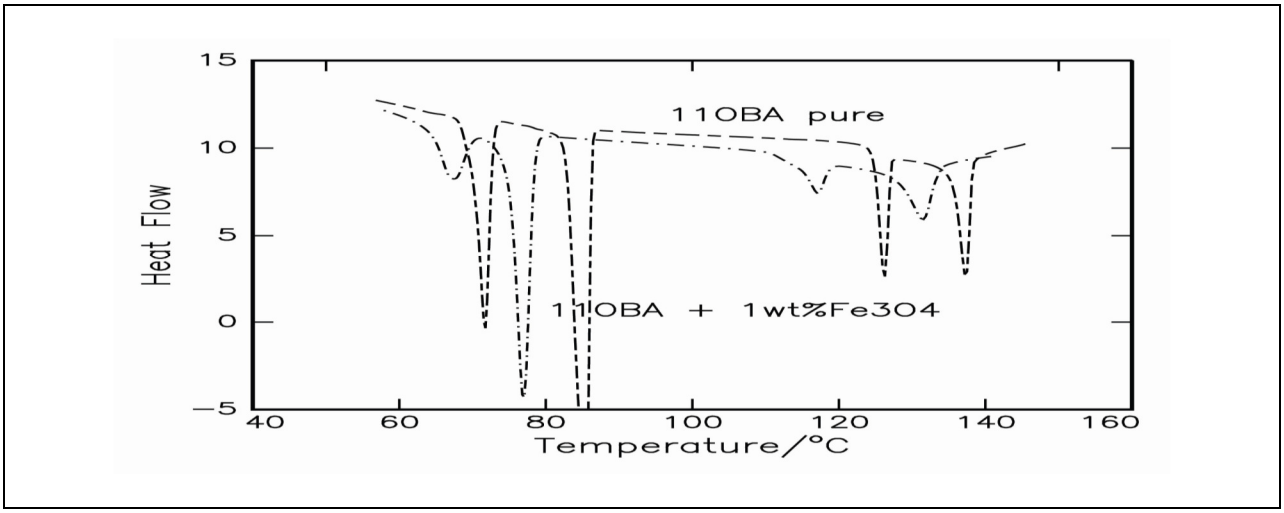

Fig.-8: DSC Thermogram of 11OBA pure & 11OBA + 1wt% Fe_3O_4 nanoparticles

FTIR Studies

As synthesized Fe_3O_4nanoparticles dispersed in 11OBA Compound is analysed by using FTIR at room temperature. The compound is stable at room temperature, the IR frequencies in solid state which are correlated in bond with the pure bond 11OBA. The assigned bonds corresponding to the resultant frequencies from the spectra are tabulated[24]. Due to the excitation of both molecular vibrations and rotations absorptions of electromagnetic radiation causes the formation of absorption bands in the IR spectra which are useful to explain the bonding interaction of the molecules.

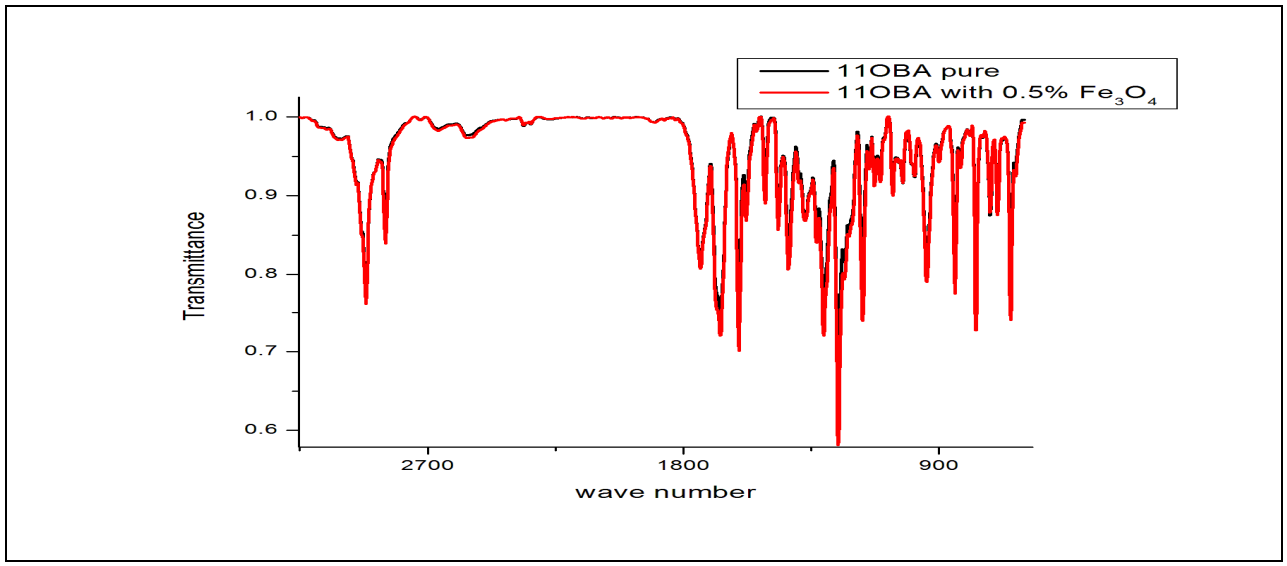

Fig.-9: FTIR analysis of 11OBA with 0.5 wt % Fe_3O_4 nanoparticles

The FTIR spectra as in Fig -9 shows the following bands for 11OBA and 11OBA doped with 0.5 wt % Fe_3O_4.A band at 2917 cm^{-1},2849cm^{-1} and 2917cm^{-1},2848cm^{-1} (O-H stretching), 1740 cm^{-1} and1740cm^{-1}(C=O), 1606 $cm^{-1}$and 1605cm^{-1} (quinoid C=C stretching), 1512 $cm^{-1}$and 1511cm^{-1} (benzenoid C=C stretching), 1466 cm^{-1} and 1466 cm^{-1} (stretching of aromatic ring), 1430cm^{-1} and 1428cm^{-1} (dimer), 1373cm^{-1} and 1373cm^{-1}(C-H stretching)[25], 1166$cm^{-1}$and 1168cm^{-1}(CH-OH bending), 1128cm^{-1},1063cm^{-1} and 1128cm^{-1} and 1063 cm^{-1} (aromatic C-H in plane bending), 843 cm^{-1}, 770$cm^{-1}$and 843cm^{-1}, 770 cm^{-1}(C-H out of plane bending) 649cm^{-1} and 647cm^{-1}confirms the existence of OH bond[26]. The transmittance of radiation has decreased in case of LC dispersed with Fe_3O_4 nanoparticles. The transmittance at peak 984cm^{-1} has decreased indicates the presence of metal oxygen vibration mode[27].

SEM Studies

A small amount of Fe_3O_4 nanoparticles dispersed LC compounds are taken on sample holder for the scanning electron microscopy. The SEM provides the investigator with a highly magnified image of the surface of a material as the present sample contains electrons; which are needed for getting SEM image. The resolution of the SEM can approach a few nm and it can operate at magnifications that are easily adjusted from about 10×-300,000×. SEM gives not only topographical information but also gives the information regarding the composition of the elements in the material[28,29]. To characterize the hypothesis of the size and shape of Fe_3O_4 nanoparticles, SEM was performed and it was shown in Fig.-11. The presence and composition of nanoparticles in the compound is be confirmed from Energy-Dispersive X-ray analysis (EDS) and shown in Fig.-10.EDS data elucidates the presence of Fe_3O_4 nanoparticles in the compound is well established.

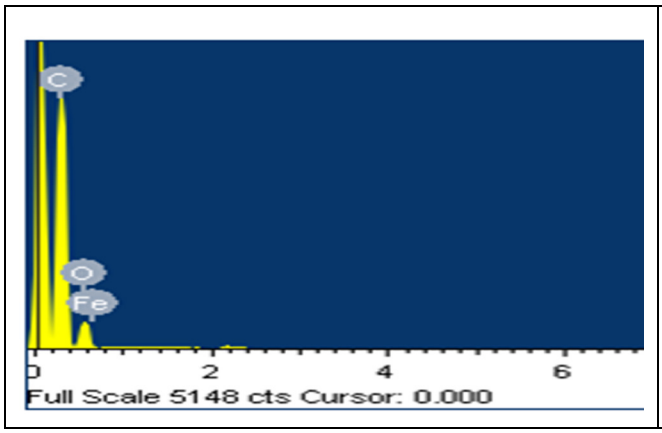

Fig.-10:EDS data of 11OBA+0.5wt% Fe_3O_4

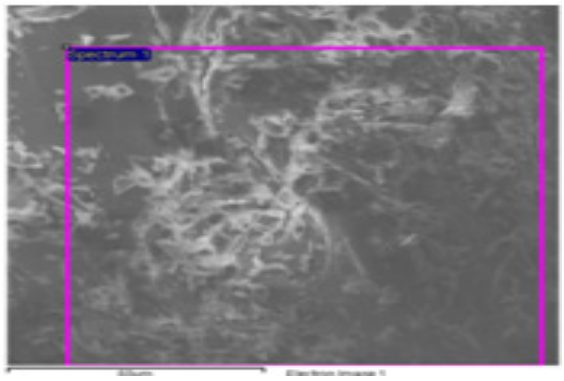

Fig.-11:SEM analysis of 11OBA+0.5wt% Fe_3O_4

Element	Weight%	Atomic%
C K	79.90	83.89
O K	20.57	16.21
Fe L	-0.47	-0.11

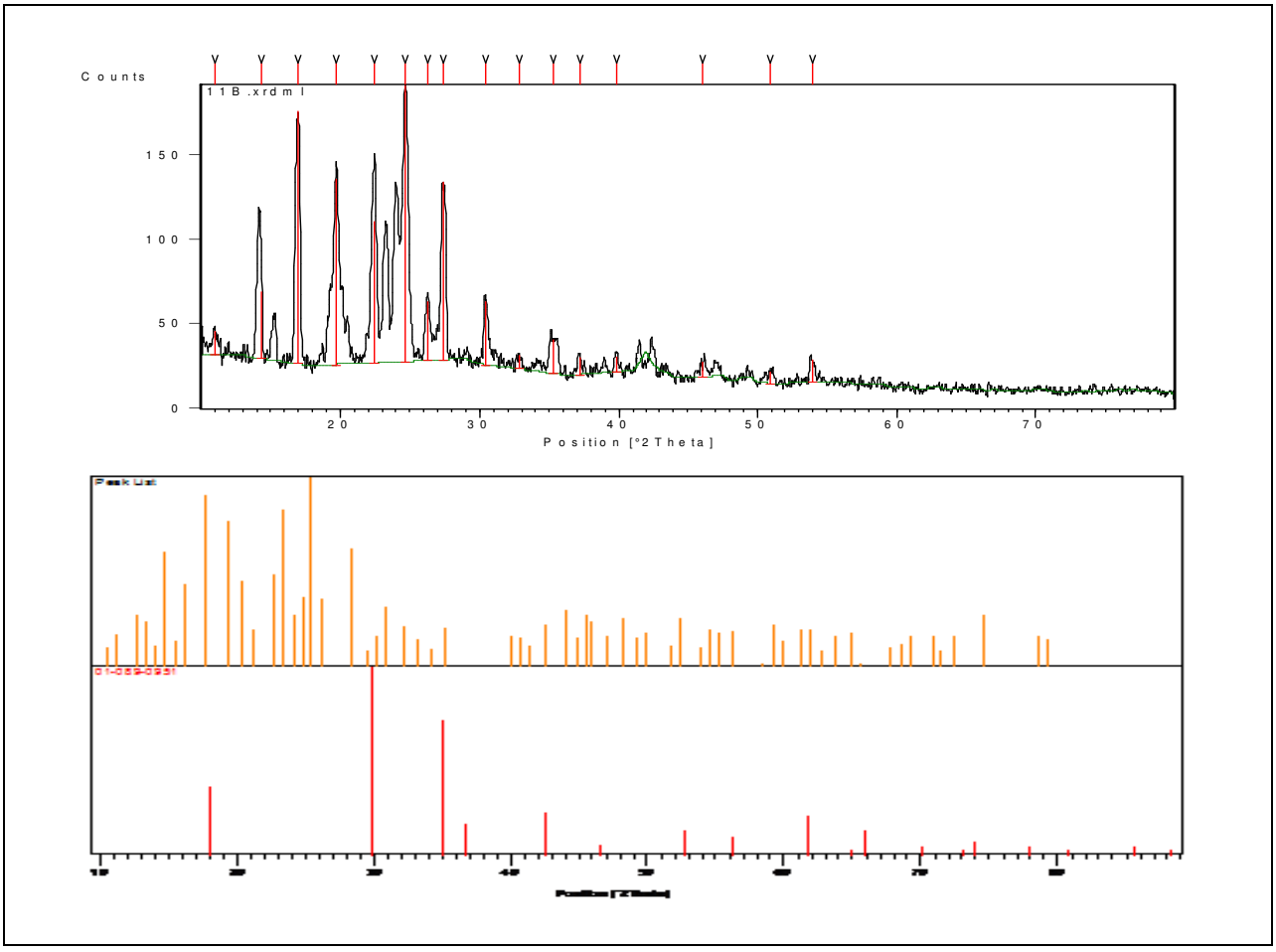

Fig.-12: XRD Analysis of 10OBA + 1wt%Fe_3O_4

XRD Studies

The XRD data of 10OBA pure and with 1wt% Fe_3O_4 nanoparticles are shown in Fig.-12in comparison of JCPDF data peaks are well resolved and are matched with JCPDF card no. 01-089-0951which is clearly evidenced the existence of Fe_3O_4 nanoparticles. By using Scherrer's Formula, $t = k\lambda/ \beta \cos\theta$, grain size is found to be 47nm, Λ=1.54 A^o, β= FWHM, Peaks at 29.57^o, 35.26^o, 42.55^o, 56.29^o, 61.95^o and 64.95^o resembles the existence ofFe_3O_4 nanoparticles which is matching with the early reporting[30-32].

Image Enhancement Studies

Image enhancement techniques bring out the detail in an image that is obscured or highlight certain features of interest in an image. Enhancement techniques include contrast adjustment, filtering, morphological filtering and deblurring. Image enhancement operations typically return a modified version of the original image and are frequently used as a pre-processing step to improve the results of image analysis techniques[33-36]. In this work adaptive histogram equalization is used to enhance the image quality (Fig.-13 to Fig.-16).

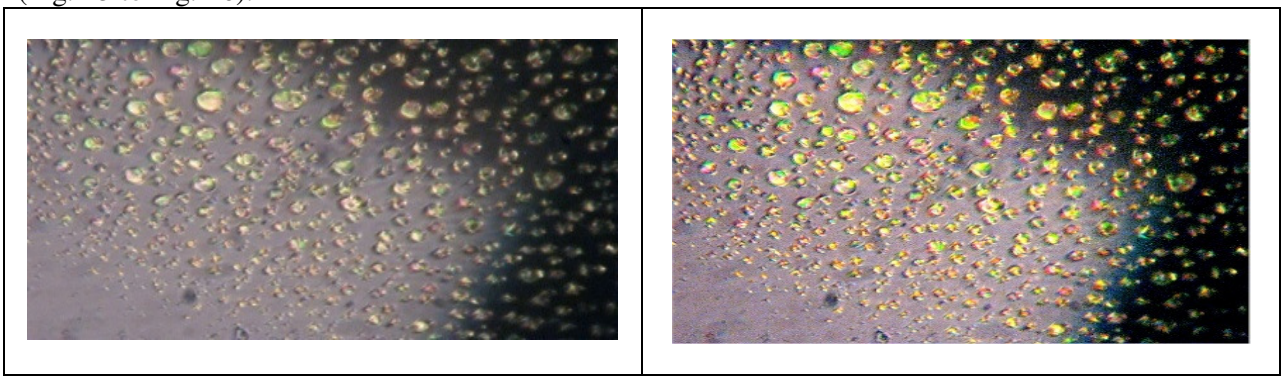

Fig.-13: Pure 10OBA nematic image and enhanced image by adaptive histogram equalization

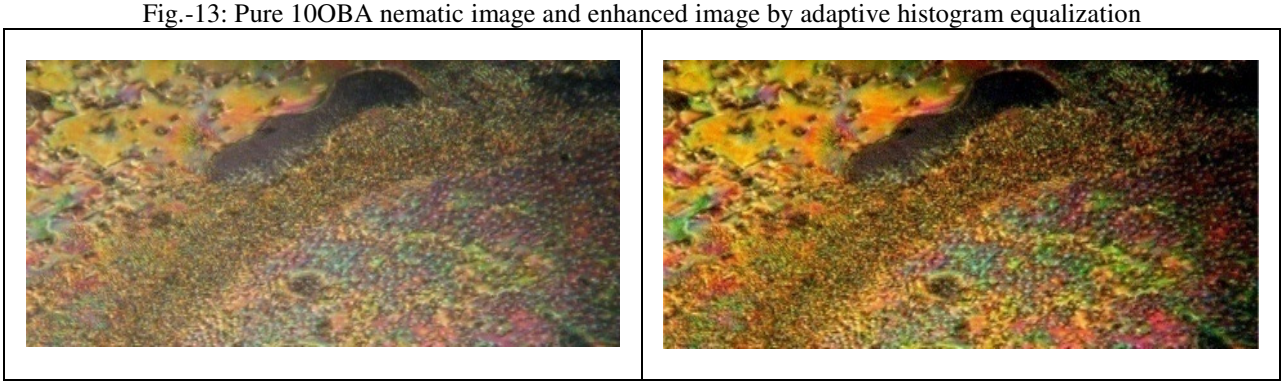

Fig.- 14: Pure 10OBA smectic-c image and enhanced image by adaptive histogram equalization

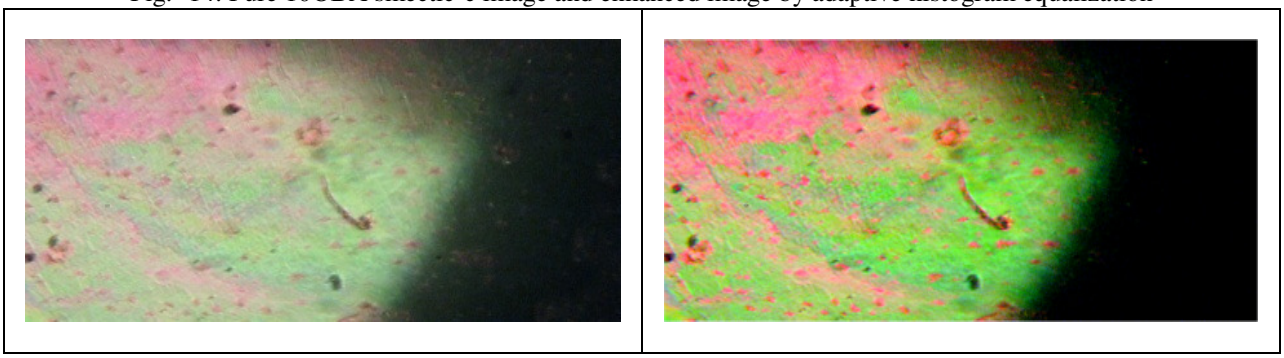

Fig.- 15: Pure 10OBA Smetic-C- Solid image and enhanced image by adaptive histogram equalization

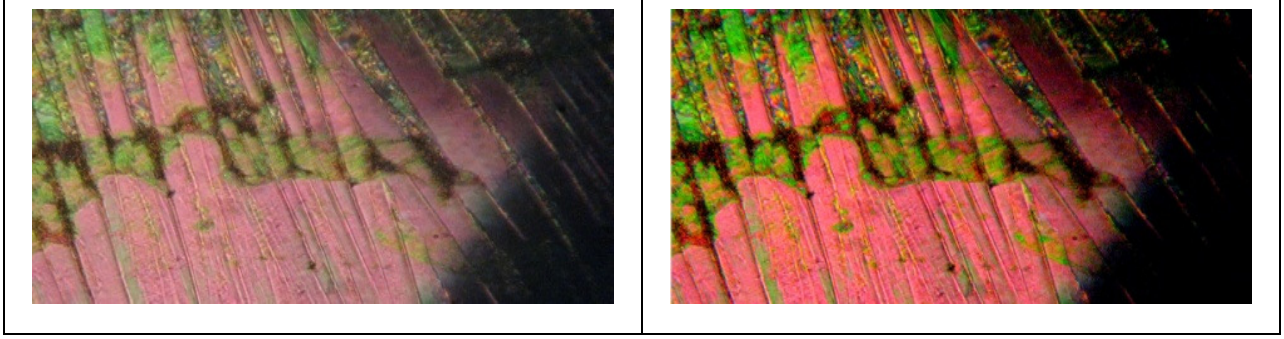

Fig.- 16: Pure 10OBA solid at 85.5^{0}C image and enhanced image by adaptive histogram equalization

Adaptive histogram equalization (AHE) improves on this by transforming each pixel with a transformation function derived from a neighbourhood region. This image enhancement is an additional work which we carried to have a clear picture on the image at transition temperatures to identify the phase very easily.

CONCLUSIONS

From these studies on 10OBA and 11OBA liquid crystal compound with dispersed Fe_3O_4nanoparticles, transition temperatures obtained from POM attached with the hot stage are in good agreement with those obtained from DSC. The slight differences can be attributed due to the different experimental conditions. The nematic thermal ranges are slightly increased due to the dispersion of Fe_3O_4 nanoparticles. From FTIR analysis the intensity of 11OBAwith dispersed Fe_3O_4 nanoparticles are found be decrease; this related to the change in dipole that occurs during the vibration.

The vibrations that produce small change in dipole result in a less intense absorption than those result in a relatively modest change in dipole. The presence of Fe_3O_4 nanoparticles is evidenced from SEM and XRD analysis. By these studies it is clear that orientation changes with the nanoparticle dispersion will modify the transition temperature as well as textural changes which are be useful for the display applications in low temperatures. Image enhancement is also performed in this work to have clear picture on the image at transition temperature.

ACKNOWLEDGEMENTS

The author R.K.N.R. Manepalli is thankful to the UGC for grant 42-784/2013 (SR). The authors would like to express their deep gratitude towards The Hindu College, Machilipatnam and the Department of ECE, K. L. University, Guntur for their continuous support and encouragement during this work.

REFERENCES

1. T. Kato, N. Mizoshita and K. Kishimoto, *Angew, Chem., Int. Ed.*, **45**, 38 (2006).
2. J. W. Goodby, I.M. Saez, S. J. Cowling, V. Gortz, M. Drapper, A. W. Hall, S. Sia, G. Cosquer, S.E. Lee and E. P. Raynes, *Angew. Chem., Int.E.*, **47**, 2754 (2008)
3. C. Tschiersle, *Chem.Soc.Rev.*, **36**, 1930 (2007).
4. D. Demus, J. Goodby, G. W. Gray, H. W. Spiess and V.Vill, Handbook of Liquid Crystals, Wiley-VCH, Weinheim, Germany, 1(1998).
5. S. Kumar, *Synth, React, Inorg., Met.Org., Nano-Met. Chem.*, **37**, 327 (2007).
6. T. Hegmann, H. Qi and V. M.Marx, *J.Inorg. Organomet.Polm, Mater.*,**17**, 483 (2007).
7. P.G. de Gennes and J. Prost, The Physics of Liquid Crystals, second ed., Clarendon,Oxford(1993)
8. K. Takatoh, M. Hasegawa, M. Koden and M. Sakamoto, AlignmentTechnologies and Application of Liquid Crystals Devices, Taylor & Francis, New York(2004).
9. Y. Garbovskiy and I. Glushchenko, *Crystals* **5**, 501(2015).
10. P. Goel, M. Arora and A. M. Biradar,*J.App. Phy.,***115**, 124905 (2014).

11. J. B. Silva, W.D. Brito and N. D.S. Mohallem, Mater. Sci.Engg. B,**112**, 182 (2004).
12. S. Sun, C.B. Murray, D. Weller, L. Folks and A. Moser, *Science,***287**, 1989 (2000).
13. S. Sun, *Adv. Mater.,***18,** 393(2006).
14. Q.A. Pankhurst, J. Connolly, S.K. Jones, J. Dobson, *J. Phys. D Appl. Phys.,***36**, 167 (2003).
15. T. Neuberger, B. Schöpf, H. Hofmann, M. Hofmann and B.V.Rechenberg, *J. Magn. Magn.Mater.,***293**, 483 (2005).
16. D. Portet, B. Denizot, E. Rump, J.J. Lejeune, P. Jallet, *J. Colloid Inter. Sci.,***238**, 37 (2001).
17. A. Ito, M. Shinkai, H. Honda and T. Kabayashi, *J. Biosci. Bioeng.,***100**, 1 (2005).
18. X. Meng, H. Li, J. Chen, L. Mei, K. Wang, X. Li, *J. Magn. Magn. Mater.,***321**, 1155 (2009).
19. Z. Zi, Y. Sun, X. Zhu, Z. Yang, J. Dai, W. Song, *J. Magn. Magn. Mater.,***321,** 1251 (2009)
20. L.X. Phua, F. Xu, Y.G. Ma and C.K. Ong, *Thin Solid Films*,**517**, 5858 (2009).
21. E. Kashevsky, V.E. Agabekov, I.V. Prokhorov, V.S. Ulashchik, *Particuology,***6**, 322 (2008).
22. P.V.Dattaprasad,M.Ramakrishna NancharaRao,J.Lalithakumari and V.G.K.M.Pisipati*Phy.Chem. Liquids*,**47**, 123 (2009).
23. G.W. Gray, Molecular structures and properties of liquid crystals, Academic Press (1962).
24. RKNR Manepalli, G.Giridhar, M. C. Rao,P.Pardhasaradhi, K.Sivaram andV G K M Pisipati, *Carmelight,***12(1)**, 91 (2016).
25. I. A. Sophia , G. Gopu and C. Vedhi, *J. Syn.Theory Appl.*, **1**, 1 (2012).
26. H. Yan, H.J. Wang, S. Adisasmito and N. Toshima, *Bull.Chem. Soc.Japan,* **69**, 2395(1996).
27. K.S. Balaji, B. Lawrence, A. Saranya, J. Pandiarajan, N. Prithvikumaran and N.Jeyakumaran, *Int. J. Tech. Res.Appl.*,**38**, 41(2008).
28. J.I. Goldstein, D. E. Newbury, P.Echlin, D. C. Joy, C. Fiori and E. Lifshin, Scanning Microscopy and X-Ray Microanalysis, Plenum Press, New York(1981)
29. D. Newbury, D. C. Joy, P. Echlin, C. E. Fiori and J.I. Goldstein, Advanced Scanning Electron Microscopy and X-Ray Microanalysis, Plenum Press, New York(1986).
30. H.E. Ghandoor , H. M. Zidan , M.M.H. Khalil and M.I.M. Ismail,*Int. J. Electrochem. Sci.*, **7**5734 (2012).
31. G.Oskam, J. *Sol Gel Sci.Techn.*,**37**, 161 (2006).
32. S.A. Kulkarni, K.P.S. Sawadh,W.K.K. Kokate, *Int. Conf.Benchmarks Engg. Sci.Tech*., (2012).
33. M.Rambabu, K. R. S. Prasad, M.VenuGopala Rao, B. T. P. Madhav and V. G. K. M. Pisipati, *Liquid Crystals Today*, **24**, 81(2015).
34. B.T.P. Madhav, P. Pardhasaradhi, R.K.N.R. Manepalli and V.G.K.M. Pisipati, *Phase Transitions,* 1025781 (2015).
35. B.T.P. Madhav, P. Pardhasaradhi, R.K.N.R. Manepalli and V.G.K.M. Pisipati, *Liquid Crystals*,**101**,2752 (2015).
36. B.T.P. Madhav, P. Pardhasaradhi, R.K.N.R. Manepalli, P.V.V. Kishore and V.G.K.M. Pisipati, *Liquid Crystals*,37 (2015).

[RJC-1485/2016]